THREE DIMENSIONAL PANORAMIC FAST FLUORESCENCE IMAGING OF CARDIAC ARRHYTHMIAS IN THE RABBIT HEART

Fujian Qu, Vladimir P. Nikolski, Cindy Grimm, and Igor R. Efimov

Washington University, Saint Louis, Missouri

ABSTRACT

Cardiac high spatio-temporal optical mapping provides a unique opportunity to investigate the dynamics of propagating waves of excitation during ventricular arrhythmia and defibrillation. However, studies using single camera imaging systems are hampered by the inability to monitor electrical activity from the entire surface of the heart. We have developed a three dimensional panoramic imaging system which allows high-resolution and high-dynamic-range optical mapping from the entire surface of the heart. Rabbit hearts (n=4) were Langendorff perfused and imaged by the system during sinus rhythm, epicardial pacing, and arrhythmias. The reconstructed 3D electrical activity provides us with a powerful tool to investigate fundamental mechanisms of arrhythmia and antiarrhythmia therapy in normal and diseased hearts.

1. INTRODUCTION

Cardiac optical mapping, in which myocardial electrical activity is simultaneously recorded from hundreds or thousands of sites, has made great strides in furthering our understanding of the initiation, maintenance, and termination of arrhythmias.[1] The fundamental mechanism underling fluorescence is the Jablonski diagram which illustrates the processes involved in the creation of an excited electronic singlet state by optical absorption and subsequent emission of fluorescence. Optical mapping uses voltage-sensitive dyes as a means to map not only activation, but repolarization as well, when heart motions are suppressed either mechanically or pharmaceutically. Voltage-sensitive dyes, when excited, provide an optical signal reproducing an action potential and thus allow the visualization of both the activation and recovery processes in any region under view. In contrast to electrode recording techniques, optical mapping is optically isolated from extremely strong electric fields applied during the defibrillation shock. Therefore, it is a powerful tool for elucidating the exact physiological mechanisms of arrhythmia and defibrillation.

The prototype of cardiac optical mapping is monocular based. The mapped region is limited to the field of view of the optical sensor. In cardiac arrhythmias, the core of the tornado-like arrhythmia pathway can be unstable and move from one place to another. Thus a study using monocular imaging system can not collect the full information during arrhythmia if the core of reentry leaves the field of view or a reentry core is not even visible by the field of imaging. This limitation strongly motivated the efforts to build panoramic imaging systems which could record the electrical activity on the entire ventricular epicardium before, during, and after the defibrillation shock. Currently there are two available panoramic imaging solutions. In a study by Bray et al.[2], electrical activity was optically mapped using a charge-coupled device (CCD) camera and a panoramic mirror arrangement to obtain full ventricular epicardium view. Kay et al. [3] extended Bray et al.'s idea to a panoramic optical mapping system capable of imaging large hearts, which used two CCD cameras and two mirrors to obtain four views separated 90◦ apart. Nevertheless, these CCD based panoramic imaging solutions are not suitable for the study of defibrillation which requires extremely high signal quality and sample rate in order to record the short duration (in ms range) shock-induced membrane potential changes. Compare to CCD cameras, photodiode array (PDA)-based imaging systems offer superior signal quality, sample rate, and dynamic range.

Moreover, many findings in defibrillation have been limited since these studies used structurally normal heart models, whereas a large percentage of patients who received defibrillation therapy actually suffered from coronary diseases such as ischemia and myocardial infarction. Vulnerability and defibrillation have not been widely studied by optical mapping at the whole heart level under these disease conditions. In this study, we developed a PDA based three dimensional fast fluorescence panoramic imaging (FFPI) system. This system is operated at 5k frames/sec sample rate and has 768 pixels in total. The reconstructed electrical activity on the entire heart surface provides us with a powerful tool to investigate mechanisms of defibrillation in normal and diseased hearts.

2. MATERIALS AND METHODS

2.1. Isolated Rabbit Heart

This study conformed to the guidelines of the American Heart Association. New Zealand white rabbits (n=4) of either gender weighing 2.7 - 3.5 kg were injected intravenously with sodium pentobarbital (50 mg/kg) and with 2000 U heparin. The hearts were quickly removed, placed on a Langendorff apparatus, and perfused with oxygenated Tyrode solution. The hearts were stained with a gradual injection of 500 µl of stock solution (1.25 mg/ml) of the voltage-sensitive dye di-4-ANEPPS in dimethylsulfoxide (DMSO), delivered by a micro pump over 5 min. The excitation-contraction uncoupler 2,3-butanedione monoxime was added to the perfusate to suppress motion artifact in the optical recordings.

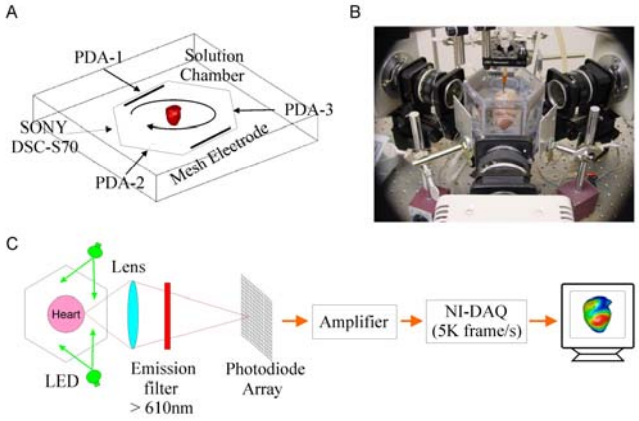

2.2. Fast Fluorescence Panoramic Imaging System (FFPI)

Shown in Figure 1A-B, 3 PDAs (Hamamatsu, Japan) spaced 120◦ apart were positioned toward the center of the solution chamber, the other 3 projections were used for excitation light illumination by commercial available light emitting diode (LED) arrays (Luxeon Flood). To mimic the configuration of external defibrillation, two stainless steal mesh electrodes were put into the solution chamber in an orientation perpendicular to the projection of PDA-1. The right ventricle faced PDA-1 and the left ventricle faced the mesh electrode distant from PDA-1. The perfusion cannula was connected to a rotation stage. A digital camera was used to take images of the heart (640 × 480 pixels resolution) while the stage was rotated around its axis. These images were used to reconstruct the 3D heart geometry. As shown in Figure 1C, for each individual PDA, the fluorescence emitted from the heart was filtered using an emission filter (>610 nm), and collected by a PDA with built-in first-stage preamplifiers. The outputs of the PDA were fed into a 256 channel second-stage amplifier and then recorded by a data acquisition system (National Instrument PXI-1006 and DAQ 6071E) operated at 5k frames/sec.

2.3. Camera Model

A commonly accepted camera calibration model, the so-called affine distortion model, states that a 3D-point M ($M = [X, Y, Z]^T$) is projected with a perspective projection onto an image plane on a 2D-point m ($m = [\mu, \nu, 1]^T$) based on the projection equation:

$$\lambda \begin{bmatrix} \mu \\ \nu \\ 1 \end{bmatrix} = \begin{bmatrix} f_\mu & \gamma & \mu_0 \\ 0 & f_\nu & \nu_0 \\ 0 & 0 & 1 \end{bmatrix} \begin{bmatrix} X \\ Y \\ Z \end{bmatrix} \quad (1)$$

Where f_μ and f_ν are the focal distance expressed in units of horizontal and vertical pixels. μ_0 and ν_0 represents the principal coordinates which corresponds to the image of the optical center. γ (skew factor) encodes the angle between the x and y pixel axes to let the camera model naturally handles non-square pixels. The digital camera we used to take pictures has square pixels so that the skew factor γ was known to be 0. We used this model for heart surface reconstruction and texture mapping, described below.

2.4. Heart Surface Reconstruction

The occluding contours algorithm [4] has been used in previous panoramic imaging study by Bray et al. [2] as the principle method to reconstruct heart surface geometry. The essence of occluding contours method is to iteratively shave a 3-D cube by silhouette edges to obtain the volume of an object inside this cube. Kay et al. [3] incorporated an adaptive octree mesh refinement algorithm into the occluding contours method to reduce computational load and memory requirements. We implemented these algorithms which proceed as follows:

1) The digital camera is positioned at a fixed distance from the solution chamber while its optical axis is aligned with the axis of rotation of the rotation stage. After we solve the intrinsic parameters of the camera model, we take 72 images (0.12 mm/pixel resolution) of the heart while the rotation stage rotates around its axis for a full 360° revolution with a 5° rotation step.
2) The heart boundary in these images was extracted by a combined image processing procedure including intensity adjustment, intensity thresholding, image opening and image closing. After heart boundary detection, we create silhouettes (72 in total) for these images by setting the pixels on the heart to value 1 and the rest of pixels to value 0.
3) A 3-D cube just large enough to contain the heart is created. The cube is initially divided into 8 voxels.
4) The voxel vertices are projected to the camera imaging plane based on equation (1) to determine their silhouette value (α) using bilinear interpolation of the silhouette image at the rotation angle. The value of α of a single vertex is clamped to 0 if α is equal to 0. We then rotate the cube 5° around the axis of rotation and compute α of the

vertices from the next corresponding silhouette image. This procedure is repeated for all the silhouette images. Now voxels that have all 8 corners outside the heart volume ($\alpha < 0.95$) and voxels have all 8 corners inside the heart volume ($\alpha \geq 0.95$) are excluded from further analysis.

5) For the remaining voxels, each of them is further evenly divided into another 8 voxels and repeats step 4). The entire process is repeated until the desired resolution is achieved (≈ 0.2mm). The centroid of these voxels forms a set of scattered points approaching the heart surface.

We then reconstructed the heart surface by an advanced algorithm called analytic surface reconstruction from points. In this approach we cover the point set with overlapping charts. Each chart is a polynomial function fit to a connected subset of the points. The individual chart functions are then blended together to produce the surface with guaranteed spherical topology. Any gaps due to missing data are filled in by adding additional charts. Unlike previous reported approaches [5], this method do not require any a priori model, nor do we rely on projection to establish a correspondence between the data points and the surface. Once the surface is reconstructed it can be tessellated at any desired resolution with near-equilateral triangles. The charts also provide a local parameterization for every point on the surface, suitable for use in, e.g., texture mapping and representing other data on the surface.

2.5. Texture Mapping and 3D Visualization

The next step is texture mapping the optically recorded action potential onto the reconstructed heart surface mesh. We develop a robust algorithm to assign such data to each element in the surface mesh:

1) Register mesh to PDA projections: The reconstructed heart surface mesh is registered to the PDA projections by calculating the visible angle between the outward normal vector (n) of each mesh cell and each normalized PDA projection vector (p). Then we define the projection angle (Φ) as:

$$\phi = \cos^{-1}(\vec{n} \bullet \vec{p}) \times \frac{180}{\pi} - \frac{\pi}{2} \qquad (2)$$

Cells visible from a particular view have projection angles greater than 0◦ for that view. The view with the maximum projection angle at 90◦ for a cell provides the best vantage point for viewing the surface of the cell.

2) Single or dual projection texture mapping: The texture mapping procedure depends on the registration of mesh cells. For each cell registered to a single PDA projection, its centroid is back projected onto the corresponding PDA imaging plane to determine the action potential value using bilinear interpolation. This action potential value is used as the fluorescent amplitude of the cell. For each cell registered to two PDA projections, the same procedure is performed twice but for different PDA projections. We then compute the weighted average value as the fluorescent amplitude of the cell based on the following equation

3) Fluorescent signals were scaled to mV assuming that a normal resting potential of -85 mV and action potential amplitude of 100 mV were present at all of the mesh cells.

4) We perform 3-D visualization in MATLAB using multi-faceted patches method.

2.6. Experiment Protocol and Data Analysis

A bipolar Ag-AgCl pacing electrode with 1 mm inter-electrode distance was placed at the anterior epicardium. We first recorded sinus rhythm, then the heart was paced and the electrical activity during this epicardial pacing was recorded. After the pacing stimuli, a test shock was delivered to the heart through the mesh electrodes spaced 100 mm apart inside the solution chamber. Shocks were delivered using a custom made defibrillator. Arrhythmias were introduced by either burst pacing from the bipolar pacing electrode or a T-wave shock. Sustained arrhythmias were recorded and then an extra shock was delivered to restore the normal rhythm.

The signal to noise ratio (SNR) presented in this paper is peak-to-peak SNR. We select a single beat of sinus rhythm, peak to peak amplitude of noise is computed during action potential phase-0 (diastole), and peak to peak amplitude of florescent action potential is computed during action potential systole.

3. RESULTS

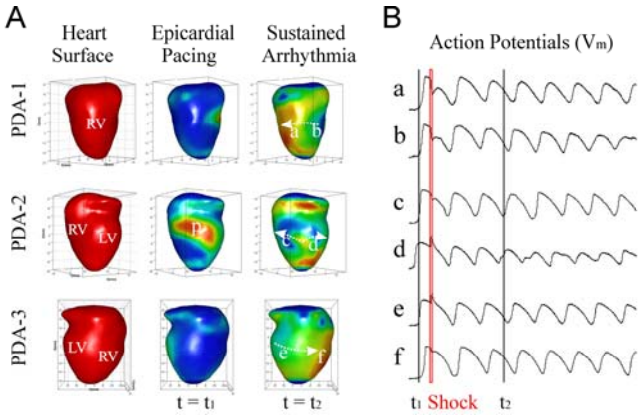

Figure 2A shows an example of the reconstructed heart surface and epicardial action potential texture mapping. In panel A, Left: the reconstructed heart surface; Middle: epicardial action potential texture mapping when heart was paced by an epicardial pacing at location p; Right: epicardial action potential texture mapping during shock-induced ventricular tachycardia. Signals from locations a-f are shown in panel B. The heart was first ventricular paced (t = t1, shown in panel A middle column), then a shock from two mesh electrodes was delivered at the plateau of the action potentials which induced a sustained ventricular tachycardia (t = t2, shown in panel A right column).

One potential advantage of using multiple cameras to visualize an object is that we might be able to improve the SNR in the dual visible areas. To confirm this, all the heart surface mesh cells were registered. Figure 3A shows the registration (darker grays: only visible by a single PDA, lighter grays: visible by two PDAs, black: not visible by any PDA). For all the dual registered mesh cells with projection angles Φ_1 and Φ_2, we computed two types of SNRs (SNR_O and SNR_N). SNR_O is the SNR of the fluorescence signal after weighted averaging process. SNR_N is the SNR of the fluorescence signal from a single PDA that has larger projection angle. Figure 3B demonstrates that SNR_O is larger than SNR_N in a majority of the dual registered mesh cells, which indicates that we could improve SNR by averaging the two fluorescence signals recorded by different PDAs. Also, when the absolute difference between Φ_1 and Φ_2 ($\Delta\Phi$) increased, the fluorescence signal from the PDA with the larger projection angle dominates the SNR calibration, thus the difference between SNR_O and SNR_N became smaller (shown in Figure 3B). Furthermore, Figure 3C shows the SNRs at all of the mesh cells including overlapping areas (filled circle) and non-overlapping areas (open circle), which demonstrated that our imaging system provides uniform data collection from the entire epicardium.

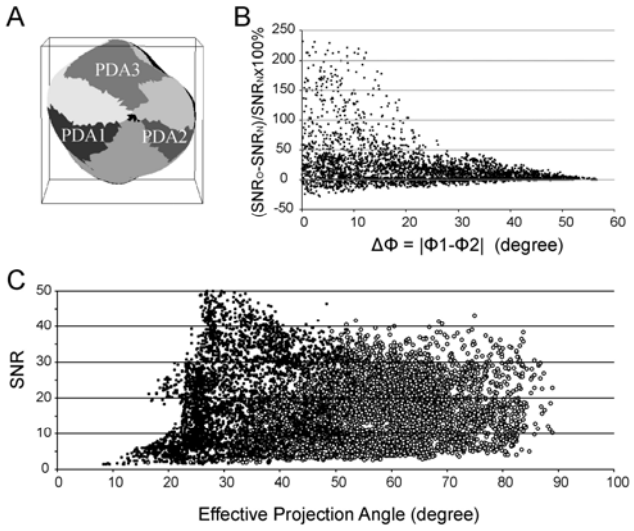

4. DISCUSSIONS

In this study we developed a novel photodiode array (PDA) based panoramic imaging system operated at 5000 frames/sec sample rate and has 768 pixels in total. The new system provides uniform data collection from the entire epicardium of a Langendorff perfused rabbit heart. One of the major advantages of this panoramic imaging system is its ability to record high signal to noise ratio (SNR) signals even when PDAs were partially obstructed by the mesh electrodes - used to deliver external defibrillation shock. Moreover, the system also shows superior quality signals when imaging a heart with healed myocardial infarction. The reconstructed 3D electrical activity provides us with a powerful tool to investigate mechanisms of defibrillation and pacing in normal and diseased hearts for complex spatial-temporal electrical field and ischemic zone configurations.

The spatial resolution of optical mapping is dependent upon the surface area mapped and the number of available pixels. In our studies, each PDA (16 by 16 pixels) imaged 760 mm^2. This area contained a small portion of the atrial epicardium and all of the ventricular epicardium. Three PDAs provided 768 pixels in total. Approximately 570 of those pixels contained data. On average, each pixel mapped an area of 2.9 mm^2, providing an average spatial resolution of 1.72 mm before the application of bilinear interpolation procedures. This spatial resolution, together with 5k frames/sec temporal resolution, is high enough for study of wavefront propagation during arrhythmias and defibrillation [6].

5. STUDY LIMITATIONS

The cardiac electrical activity is essentially a 3D phenomenon, in particular, during complex arrhythmias. Results of this study are limited due to typical penetration depth of optical mapping technique.

6. ACKNOWLEDGEMENT

This work was supported by NIH grants (HL67322, HL074283) and NSF grant 049856.

7. REFERENCES

Bibliography

[1] Efimov, I. R., Nikolski, V. P., and Salama, G.."Optical imaging of the heart," *Circ Res*, vol. 95, no. 1, pp. 21-33, July2004.

[2] Bray, M. A., Lin, S. F., and Wikswo, J. P., Jr.."Three-dimensional surface reconstruction and fluorescent visualization of cardiac activation," *IEEE Trans Biomed Eng*, vol. 47, no. 10, pp. 1382-1391, Oct.2000.

[3] Kay, M. W., Amison, P. M., and Rogers, J. M.."Three-dimensional surface reconstruction and panoramic optical mapping of large hearts," *IEEE Trans Biomed Eng*, vol. 51, no. 7, pp. 1219-1229, July2004.

[4] Niem, W.."Robust and fast modeling of 3D natural objects from multiple views," *Proc.SPIE: Image and Video Processing II*, pp. 388-397, 1994.

[5] Grimm, C., Laidlaw, D., and Crisco, J.."Fitting Manifold Surfaces To 3D Point Clouds," *Journal of Biomechanical Engineering*, vol. 124 pp. 136-140, 2002.

[6] Bayly, P. V., Johnson, E. E., Idriss, S. F., Ideker, R. E., and Smith, W. M.."Efficient electrode spacing for examining spatial organization during ventricular fibrillation," *IEEE Trans Biomed Eng*, vol. 40, no. 10, pp. 1060-1066, 1993.